Discriminating color space selection for edge detection using multiscale product wavelet transform

Sihem Charaâ and Noureddine Ellouze

**National Engineering High School of Tunis, Laboratory of Image, Signal
and Information Technology,
University Tunis El Manar, 1002,
Tunis, Tunisia.**

Abstract

Edge detection is an important low level image processing step, which can influence the final results. In this paper, an effective method, named the multiscale product wavelet transform, is proposed for edge detection. Although the one scale wavelet transform is a universal method, it is not suitable for real complex images because this method cannot efficiently detect edges. Therefore, the output edge map suffers from a considerable amount of false and double edges. An extension to the one scale wavelet transform approach is to use multiscale transform and perform the product of these scales. The use of the resulting product improves the localization of detected edges and dilutes noise. Unlike others using the multiscale transform, the proposed method applies the multiscale product wavelet transform on the most discriminating color space. This has given the best results in term of edges using a robust statistical analysis. The performance of the method is tested on a database containing 500 real images, which present very complex information.

Keywords: *Edge detection; Discriminating color space; Dyadic wavelet transform; Multiscale wavelet product; ROC analysis.*

1. Introduction

Edge detection is a low level image processing. It is a problem of contour detection. In images, contours appear as the points where great changes in brightness or color are observed, separating different objects or different conditions [1].
In this paper, we focus on detecting these contours in color images. Color is actually the human being perception of light waves from a thin band of frequencies within the electromagnetic spectrum [2]. It is a powerful descriptor that plays an important role in the aspect of digital image denotation [3]. Different color spaces have been used to represent color images.

We define the term image as a 2D light intensity function denoted by $f(x, y)$. The value or amplitude of the function f at spatial coordinates (x, y) gives the intensity (brightness) of the image at that point. Since light is a form of energy $f(x, y)$ must be non-zero and finite, i.e. $0 < f(x, y) < \infty$. A digital image $F[x, y]$ described in a 2-D discrete space is derived from an analog image $f(x, y)$ in a 2D continuous space through a sampling process known as digitization. The image colors can be represented as a set of numbers or color components; this set is called Color Space. A color space is a method by which we can specify, create and visualize color [15]. Different color spaces have been used to represent color images. In this work, to make the image edge detection more efficient the focus was put on RGB, HSV, NTSC (YIQ) and YCbCr color spaces. The RGB color space is composed of three primary additive colors: Red, Green and Blue. The additive character makes these three components highly correlated which is the main disadvantage of this representation. Another lack of the RGB space is its non-uniformity, since it is impossible to evaluate the perceived differences between colors on the basis of distances [4]. The HSV color space was developed to approximate the human interpretation of color, and it is represented by three components: Hue, Saturation and Value (intensity). It separates the color information from its intensity information. Value is achromatic and describes the brightness of the scene, while hue and saturation are the chromatic components. Hue represents the dominant color in the image since it is associated to the dominant wavelength. Saturation represents the color purity. It describes how pure the hue is with respect to a white reference [4]. The main advantages of the HSV space are its compatibility with color human perception and the distinction between chromatic and achromatic components. The YCbCr

IJCSI International Journal of Computer Science Issues, Volume 12, Issue 1, No 2, January 2015
ISSN (Print): 1694-0814 | ISSN (Online): 1694-0784
www.IJCSI.org

12

color space is extensively used in image processing. In this format, luminance information is represented by a single component, Y, and color information is stored as two color-difference components, Cb and Cr. The Cb component is the difference between the blue component and a reference value. The Cr component is the difference between the red component and a reference value. The YIQ color space is used by the NTSC color TV system, where the Y represents the NTSC luminance, and (I and Q) the chrominance color components. Edge location of people vision perception is according to lightness value and color information. The most common approach to local boundary detection look for discontinuities only in image brightness. Hence, when there is a change of color with a subtle change in brightness, a percentage of edges (almost 10%) [5] will not be detected and this will bring inconvenience to upper image processing.

Many ideas came to overcome this problem, the first output fusion method using the Hueckel's edge detector on the luminance and the two chromaticity components developed by Nevatia [6]. In Hedley and Yan [7] work, the Sobel operator was applied to the three components in the RGB space and the edge map was obtained by fusing the three gradients. Carron [8] used the HIS space to apply the Sobel operator to the hue component, taking into consideration the two other components.

In this paper, we will focus on the application of the multiscale wavelet transform to detect edges for color images. Many researchers bring their images into frequency domain from time domain, for this either they convolve or convert the image signal into wavelets domain, furthermore taking into consideration multiscale resolution at wave packet level to get more clear and detailed signal [12]. Multiresolution analysis plays a key role in the theory of wavelets. Single scale methods are used to detect edge and to suppress noise but they don't take into account the different levels of signal and noise. This technique has been used for signal processing [9, 10] and image processing. Mallat, Hwang, and Zhong [11] have proved the location of irregular structures such as edges that can be detected using the maxima of the wavelet transform modulus. Furthermore, these maxima are used to calculate Lipschitz exponents of edges that can give idea about the sharpness of an edge. Sadler and Swami [13] analyzed the multiscale products and applied them to step detection and estimation for 1-D signal. Mallat et al. [14] used the Mallat and Zhong wavelet called MZ wavelet, which approximates the first derivative of Gaussian for the multiscale edge detection.

The main reason and advantage for applying the multiscale wavelet transform to the detection of edges in an image is the possibility of choosing the size of the details that will be detected. How many edges we want to get is set by the wavelet scale.

Also, the multiscale wavelet transform is strongly anti-noise at large scales, while the small scales can accurately locate edges [16]. A trade-off between noise suppression and the preservation of actual image features has to be made in a way that amplifies the relevant image content. In this work, to make the image edge detection more efficient the focus was put on RGB, HSV, NTSC (YIQ) and YCbCr color spaces.

A comparison method is applied to select the most discriminating color space that gives best results in term of edge detection.

The remainder of this paper is structured as follows: in second section, the use of a multiscale products framework is justified. The choice of the most discriminating color space for the wavelet multiscale product edge detection is discussed in the third section. Experiments related to the proposed method are given in the fourth section in comparison with some famous edge detectors.

2. Muliscale product edge detection

Due to its capability to localize in time, the wavelet transform came as an alternative to the Fourier Transform that presented many limitations in the analysis of non-stationary signal [17, 18].

2.1 Wavelet Transform

Wavelets are mathematical functions used to dissociate data into different frequency components that appear at different resolutions. The wavelet is a square integrable function well localized in time and frequency, from which we can extract all basis functions by time shifting and scaling of the mother wavelet.

In order for the function $\psi(x)$ to satisfy the requirements to be a wavelet, it should have a compact support and n vanishing moments, i.e.

$$\int_{-\infty}^{+\infty} x^k \psi(x)dx = 0, \qquad \text{for } 0 \leq k \leq n \tag{1}$$

Suppose a differentiable smooth function $\theta(x)$ exists, with its integral equal to 1, and converges to 0 at infinity. Let's define $\psi(x)$ as the first-order derivative of $\theta(x)$,
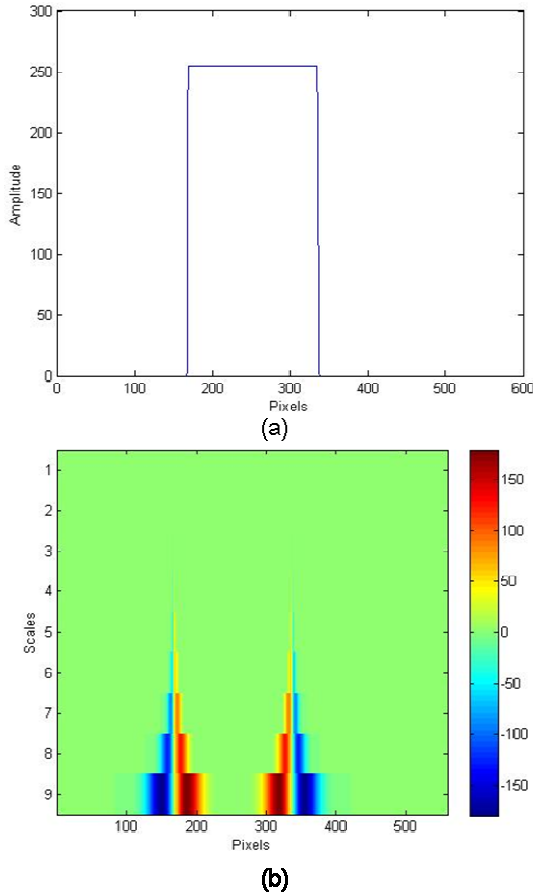
$$\psi(x) = \frac{d\theta(x)}{dx}. \tag{2}$$

Fig. 1 (a) Simulated step signal, (b) its scale/space representation, obtained through the CWT with a first derivative Gaussian mother wavelet for scales j^2, $j=1...9$.

The wavelet transform is a multi resolution representation; it decomposes a signal into a set of scales ranging from the coarsest scale to the finest one as seen in fig.1.

The continuous wavelet transform of any measurable and square-integrable function $f(x)$, $f \in L^2(\mathbb{R})$; at scale s and position x can be expressed as,

$$W_s f(x) = f * \psi_s(x) = f * \left(s \frac{d\theta_s}{dx} \right)(x) = s \frac{d}{dx}(f * \theta_s)(x) \quad (3)$$

The equation (3) shows that $W_s f(x)$ represents the first derivative of $f(x)$ smoothed by $\theta_s(x)$.

Mallat gave a 2D extension of Multiscale Wavelet Transform in [19]. For two-dimensional images, a 2D differentiable smooth function $\theta(x, y)$, with its integral equal to 1 and converges to 0 at infinity, is used.

The 2D smooth function $\theta(x, y)$ can be defined as the tensor product of two (1-D) smooth functions,

$$\theta(x, y) = \theta(x) \otimes \theta(y). \quad (4)$$

As a consequence, the wavelets $\psi^x(x, y)$ and $\psi^y(x, y)$ are generated at horizontal and vertical directions respectively, and defined as,

$$\psi^x(x, y) = \frac{\partial \theta(x, y)}{\partial x} \quad (5)$$

$$\psi^y(x, y) = \frac{\partial \theta(x, y)}{\partial y} \quad (6)$$

The wavelet transform of $f(x, y)$, which we suppose a 2D measurable and square-integrable function such that $f(x)$, $f \in L^2(\mathbb{R})$, at scale s and position (x, y) has two components:

$$W_s^x f(x, y) = f * \psi_s^x(x, y) = s \frac{\partial}{\partial x}(f * \theta_s)(x, y) \quad (7)$$

and

$$W_s^y f(x, y) = f * \psi_s^y(x, y) = s \frac{\partial}{\partial y}(f * \theta_s)(x, y) \quad (8)$$

Hence, edge points can be located from the two components $W_s^x f(x, y)$ and $W_s^y f(x, y)$ of the wavelet transform.

2.2 Multiscale Product

Mallat [19] demonstrates that the evolution across scales of the wavelet transform depends on the local Lipschitz regularity of the signal. Based on the Lipschitz regularity theorem, the link between the amplitudes and scales of the wavelet transform is presented in equation 9.

$$\left| W_{2^j} f(x) \right| \le K (2^j)^\alpha \quad (9)$$

with $0 < \alpha < 1$ and $k > 0$. As proven in [19], The Lipschitz regularity of step edge is 0. Any structure smoother than the step edge will have positive Lipschitz regularity and this is the case of singularities representing edges. For structures regular than the step edge, they have negative Lipschitz regularity and this is the case of noise. For example the Dirac function and the white noise have Lipschitz regularities equal to -1 and -1/2 respectively. Based on equation 8, this means that the wavelet transform magnitudes increase for positive α with increasing scales.

IJCSI International Journal of Computer Science Issues, Volume 12, Issue 1, No 2, January 2015
ISSN (Print): 1694-0814 | ISSN (Online): 1694-0784
www.IJCSI.org

14

Contrarily, wavelet transform magnitudes decrease for negative Lipschitz regularities with increasing scales. From this, we can conclude that the signal singularities persist across scales while the noise decays rapidly (fig. 2), hence multiplying the coefficients of the wavelet transform at adjacent scales can enhance edge structure and suppress the spurious peaks.
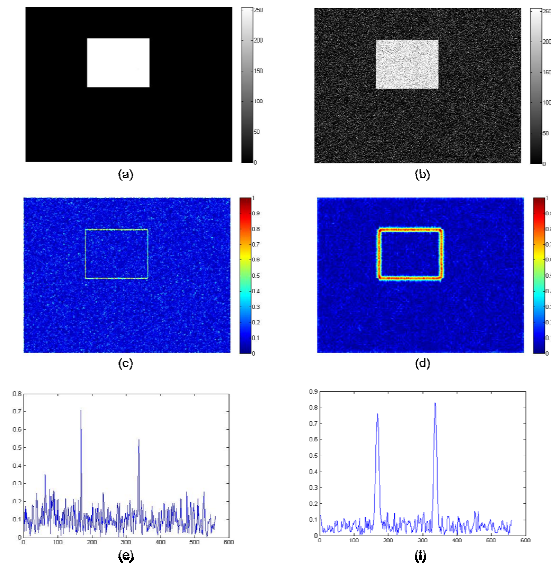
Fig. 2 Wavelet coefficients at two scales. (a) Synthetic image. (b) The image (a) contaminated with Gaussian noise of variance=0.1. (c) DWT coefficients of scale=2^0. (d) DWT coefficients of scale=2^6. (e) Horizontal cut of (c). (f) Horizontal cut of (d).

Xu et al. [20] and Sadler [21] fully exploit this magnificent conclusion in image processing to reduce noise and amplify singularities using the Multiscale Product. The multiscale product of $W_i f$ is defined in equation 10.

$$P_j f(x) = \prod_{i=k1}^{k2} W_{j+i} f(x) \qquad (10)$$

where k_1 and k_2 are non-negative integers.

For the 2-D image, the multiscale products have two components:

$$P_j^x f(x,y) = \prod_{i=-k1}^{k2} W_{j+i}^x f(x,y) \qquad (11)$$

and

$$P_j^y f(x,y) = \prod_{i=-k1}^{k2} W_{j+i}^y f(x,y) \qquad (12)$$

Before applying the wavelet transform, the type of transform and the mother wavelet should be chosen accurately. This choice is influenced by the signal to be analyzed and the type of characteristic to be focused on [22]. The use of the Continuous Wavelet Transform (CWT) in the proposed approach provides redundant information in time and scale, which is required for edge detection. Numeric images processing require the use of the Dyadic Wavelet Transform (DWT). The DWT is a version of the CWT when the scale parameter s is discretized along the dyadic grid (2^j), with $j \in IN$. The number of products is very important.

An odd number of products preserves the maxima sign and generates unbiased results [21]. Generally, the product of three levels wavelet decomposition is optimal.

3. Discriminating color space selection for multiscale product edge detection

We now introduce our own multiscale product edge detection with the choice of the most discriminating color space. The Berkeley Segmentation Dataset (BSDS500) [23] have been used for experimentation. This database is composed of 500 color images, where each image has been manually segmented by at least 5 different subjects to generate Ground Truths. These Ground Truths were used as reference to evaluate our proposed approach.

In the framework of this paper, the proposed approach has been applied on all the Berkeley Database.

As we have seen in Section 2, the wavelet transform has the capability both to localize the precise position of the edge at small scales, and to be unaffected by the noise at large scales. So, using the interscale pointwise product of several scales allow getting benefit of the good performance in the resolution of the lower ones, as well as the sensitivity to the presence of discontinuities of the higher ones.

In this paper, we propose a color image edge detection method based on the multiscale wavelet transform. This method was applied to a color image in different color spaces and a selection of the most discriminating color space was performed.

The proposed edge detector, as shown in fig. 3, consists of three main steps: the pre-processing step, the multi-scale product edge detection step and the selection of the most discriminating color space step.
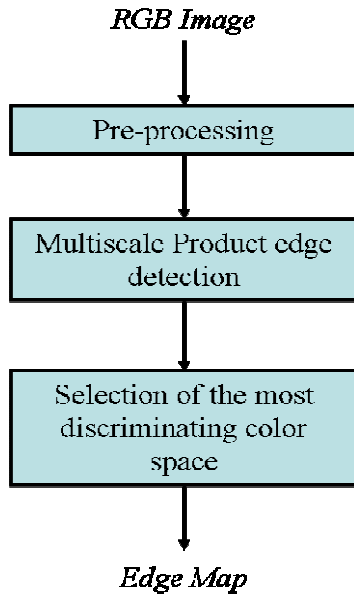
IJCSI International Journal of Computer Science Issues, Volume 12, Issue 1, No 2, January 2015
ISSN (Print): 1694-0814 | ISSN (Online): 1694-0784
www.IJCSI.org

15

RGB Image

Pre-processing

Multiscale Product edge detection

Selection of the most discriminating color space

Edge Map

Fig. 3 General diagram of the proposed method for color images.

3.1 Pre-processing step

The candidate color spaces used in this work are RGB, YCbCr, HSV and YIQ, so conversions of the initial RGB color image to YCbCr, HSV and YIQ are needed.

- The color difference from RGB to YCbCr format in which Luminance Y and the two chrominance are given by the matrix below.

$$\begin{cases} Y = 0.3\,R + 0.58\,G + 0.11\,B \\ Cb = -0.17\,R - 0.4\,G + 0.51\,B + 128 \\ Cr = 0.51\,R - 0.43\,G + 0.04\,B + 128 \end{cases} \quad (13)$$

- The color difference from RGB to HSV format in which Hue is given by

$$H = \begin{cases} \theta, & B \le G \\ 360 - \theta & B \ge G \end{cases} \quad (14)$$

where

$$\theta = \cos^{-1}(0.5((R-G)+(R-B))/(R-G)^2+(R-B)*(G-B))^{1/2})) \quad (15)$$

The saturation is given by

$$s = 1 - (3/(R+G+B)) * (\min(R,G,B)) \quad (16)$$

Finally the Value is given by

$$V = (1/3)*(R+G+B) \quad (17)$$

- The color difference from RGB to YIQ format is given by equation 18.

$$\begin{cases} Y = 0.3\,R + 0.59\,G + 0.11\,B \\ I = 0.6\,R - 0.28\,G - 0.32\,B \\ Q = 0.21\,R - 0.52\,G + 0.31\,B \end{cases} \quad (18)$$

The RGB image and its corresponding conversions in YCbCr, HSV and YIQ color spaces (fig. 4) represent the output of the pre-processing step and the input of the *MP edge detection step*.
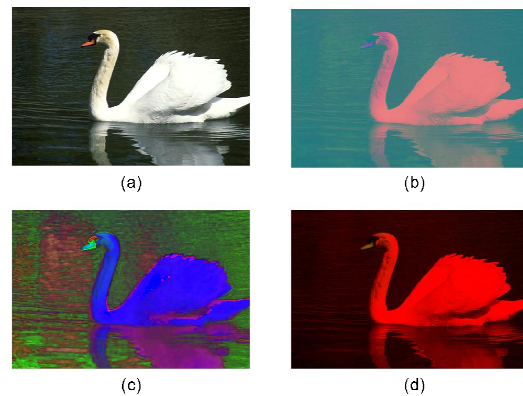

(a)

(b)

(c)

(d)

Fig. 4 Example of used BSDS images. a) RGB image, (b), (c) and (d) their conversions to YCbCr, HSV, and YIQ domains respectively.

3.2 Multiscale Product edge detection step

The proposed algorithm is applied to RGB, HSV, YIQ and YCbCr color images from BSDS database. In this work, we selected the non-isotropic first derivative of a Gaussian as a mother wavelet in the analysis. It's proportional to the first derivative of the Gaussian probability density function. The Gaussian first derivative wavelet is defined as:

$$\psi(x) = -x\exp\left(-\frac{x^2}{2}\right) \quad (19)$$

Its effective support range is [-5, 5].

The flowchart of the proposed *Multiscale Product Edge Detection* step is presented in fig. 5. The 3D color image is composed of three components. Aiming not to lose the information existing in the image, we will extract edges from every component.
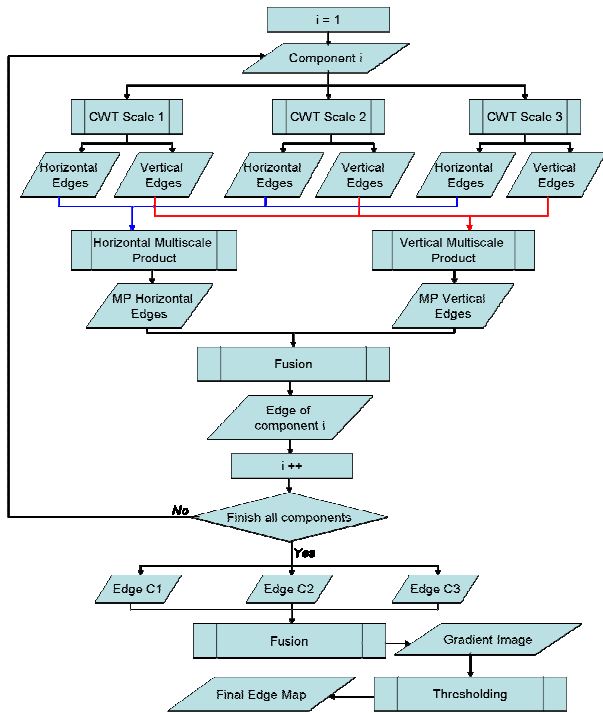
IJCSI International Journal of Computer Science Issues, Volume 12, Issue 1, No 2, January 2015
ISSN (Print): 1694-0814 | ISSN (Online): 1694-0784
www.IJCSI.org

16

Fig. 5 Flowchart of the proposed Multiscale Product edge detection step.

For each component i, three dyadic wavelet transforms are applied to lines (to get the vertical edges) and to columns (to get the horizontal edges) using three scales. The used scales are 2^1, 2^2 and 2^3 respectively (fig. 6).
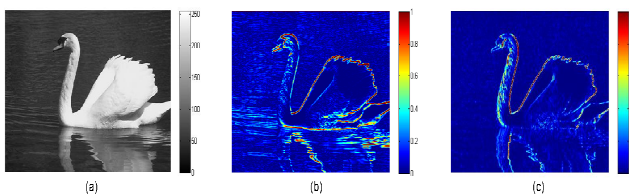

Fig. 6 Dyadic Wavelet Transform of scale=2 (a) Y component of YCbCr image. (b) Horizontal edges. (c) Vertical edges.

Then, the two pointwise products are performed to the three horizontal edges gradients and the three vertical edges gradients to get the Horizontal Multiscale Product and the Vertical Multiscale Product respectively (fig. 7 (b, c)). Next, the Horizontal Multiscale Product and the Vertical Multiscale Product are fused to get the gradient image of the component i (fig. 7 (d)).

The last steps are repeated for the two other components. The three gradient images are fused to get the final gradient image (fig. 8).
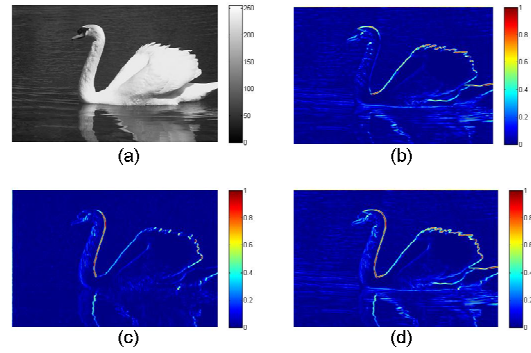

Fig. 7 Example of Multiscale Product at scales: 2, 4 and 8 of a component. (a) Y component of YCbCr image. (b) Horizontal edges. (c) Vertical edges.

Finally, the obtained Gradient Image should be thresholded to eliminate false edges produced by noise. If a single threshold t is used, for small values of t there will still be some false edges. Portions of a contour may be missed for large values of t.
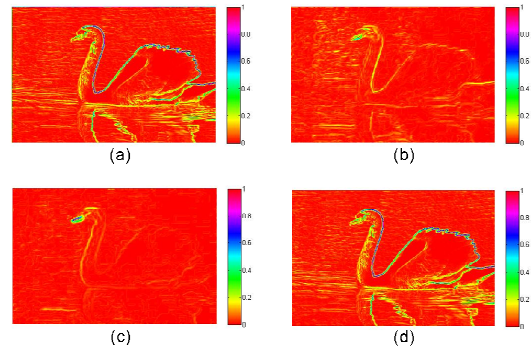

Fig. 8 Example of Multiscale Product at scales: 2, 4 and 8 of YCbCr image. (a) MP of Y component. (b) MP of Cb component. (c) MP of Cr component. (d) Fusion of edges.

Canny edge detection uses a double thresholding called "hysteresis". A low threshold and an upper threshold are applied. Considering a line segment, if a value lies above the upper threshold limit, it is immediately accepted. If the value lies below the low threshold, it is immediately rejected. Points lying between the two limits are accepted if they are connected to accepted pixels. The double thresholding algorithm can also be applied in our scheme. Since edges and noise can be better distinguished in the scale product than in a single scale, a properly chosen threshold could suppress the noise maxima effectively. Due to this observation and for simplicity the single threshold is preferred.

At the end of this step, after thresholding, we obtain four binary edge images corresponding to RGB, HSV,

IJCSI International Journal of Computer Science Issues, Volume 12, Issue 1, No 2, January 2015
ISSN (Print): 1694-0814 | ISSN (Online): 1694-0784
www.IJCSI.org

17

YIQ and YCbCr images respectively. Examples of final edge maps are shown in fig. 9.
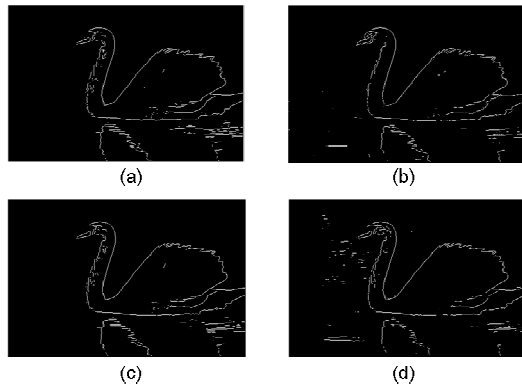

(a)

(b)

(c)

(d)

Fig. 9 Final edge map images. (a) RGB edge map. (b) HSV edge map. (c) YCbCr edge map. (d) YIQ edge map.

After applying the preprocessing and the multiscale product edge detection steps to the 500 images composing the BSDS database, we get 2000 (500*4 color spaces) binary edge images.

3.3 Selection of the most discriminating color space step

In order to determine between RGB, HSV, YIQ and YCbCr which color space is the most discriminating one giving the best results in term of edge detection using Multiscale Product Wavelet Transform, we will use the Receiver Operating Characteristic (ROC) analysis, which was first introduced in [24].

The ROC curves are commonly used to present results for binary decision problems. By comparing the marked pixels provided by a classification method, four cases are available as shown in the confusion matrix (table 1).

Table 1. Confusion matrix of ROC analysis.

		Pixels assigned to the class ω_i (i=1,2) in $\mathbf{I_{ref}}$	
		ω_1	ω_2
Pixels assigned to the class ω_i (i=1,2) in I	ω_1	True Positive (TP)	False Positive (FP)
	ω_2	False Negative (FN)	True Negative (TN)

Where, I denotes the binary image resulting from the edge detector; and I_{ref} denotes the reference image Ground Truth, which contains the true edges marked by experts. The edge detector tries to detect edges that can be classified into four categories: True Positive (TP),

False Positive (FP), True Negative (TN), and False Negative (FN). The TP-Edge pixel in an image is detected correctly as edge pixel. The FP-Non edge pixel is detected wrongly as edge pixel. The TN-Non edge pixel is detected correctly as non edge pixel. The FN-Edge pixel is detected wrongly as non edge pixel.

The principal ROC analysis parameters are [25]:

- True Positive Rate (TPR), or *Sensitivity*, given as $TPR = TP/(TP + FN)$.
- False Positive Rate (FPR), defined as $FPR = FP/(FP + TN)$.
- True Negative Rate (TNR), or *Specificity*, given as $TNR = 1 - FP$.
- *Accuracy*, in percentage, obtained by $Accuracy = ((TP + TN)/(TP + TN + FP + FN)) * 100$.
- Performance Ratio (PR), calculated by $PR = (TP/(FP + FN)) * 100$.

The ROC curve gives a view of all the True Positive Rate/False Positive Rate pairs generated from varying the correspondence over the range of observed data [26].

The results of the proposed approach will be evaluated using the above formulas. The ROC curve has been generated for each of the resulting edge map images, where the ROC curve represents the plot of the True Positive Rate (Sensitivity) against the False Positive Rate (1-Specificity) for different thresholds (fig. 10).

Furthermore, for each of the four color spaces, an average ROC plot has been generated for the corresponding edge map images (fig. 11). Each point on the ROC curve represents a Sensitivity/Specificity pair corresponding to a particular decision threshold.

The comparison between the four average ROC plots (fig. 11), resulting from the previous step, is enabled to select the color system that would provide an optimal trade-off between the True Positive Rate and the False Positive Rate. This optimal trade-off should be the closest to the upper left corner, where the FPR is the lowest and the TPR is highest. Among the four color spaces, the RGB and YCbCr show the best results. However, the ROC curves of the RGB and YCbCr spaces were found to be superimposed, which makes difficult to compare between both of them. Therefore, in order to make the comparison possible, we used the accuracy versus threshold as an additional plot. Similarly, for every edge map image for RGB and YCbCr color spaces we plot the Accuracy against threshold (fig. 12).

IJCSI International Journal of Computer Science Issues, Volume 12, Issue 1, No 2, January 2015
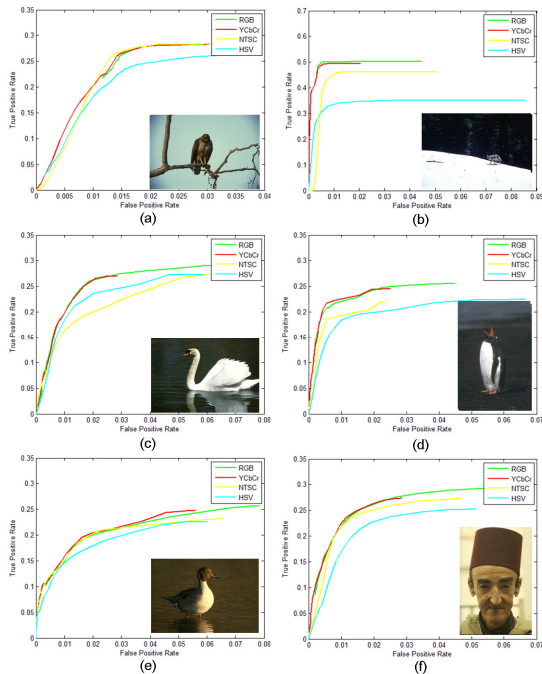ISSN (Print): 1694-0814 | ISSN (Online): 1694-0784
www.IJCSI.org

18

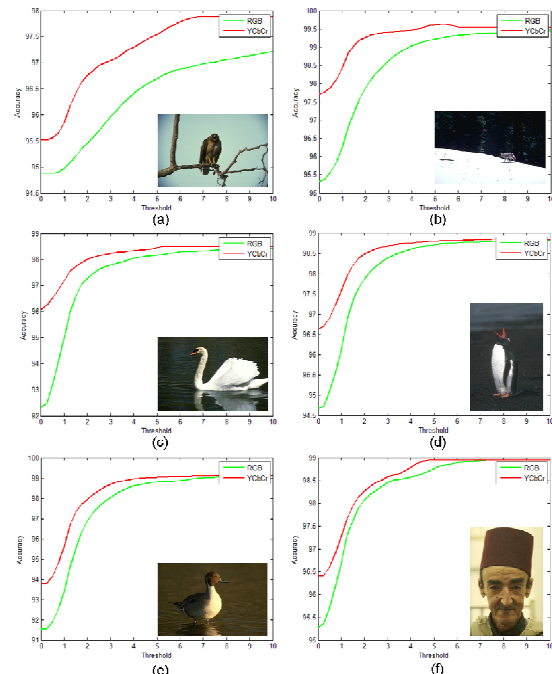Fig. 10 Example of BSDS images and their TPR vs. FPR plots for different color spaces

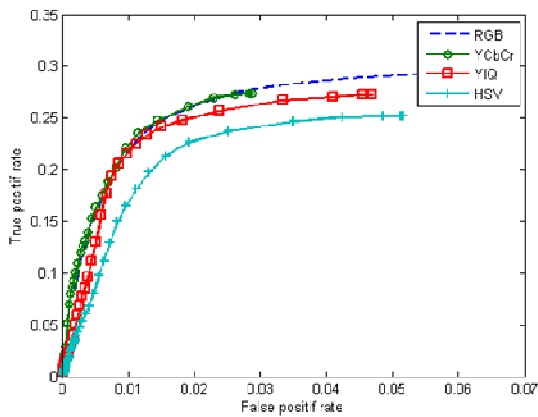Fig. 12 Example of BSDS images and their Accuracy vs. Threshold plots in YCbCr and RGB color spaces.

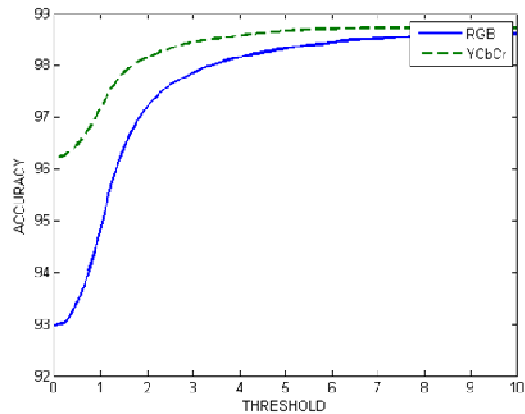Fig. 11 Average TPR vs. FPR plots for different color spaces.

Fig. 13 Average Accuracy vs. Threshold plots for YCbCr and RGB color spaces.

The Accuracy represents the percentage of true detected edges. Fig. 13 shows Accuracy versus Threshold plots of the average of the edge map images in the RGB and YCbCr spaces. Similarly to the TPR vs. FPR plot, the best result is the one belonging to the color system, with trade-off the nearest to the upper left corner. Consequently, the best result was found to be the YCbCr system, which was elected to be used subsequently for the proposed approach evaluation.

4. Evaluations and results

To provide a basis of comparison for our algorithm we use Canny [27], Sobel [28] and Prewitt [29] edge detectors. We evaluate each method using two parameters: The Performance (PR), which represents the ratio of true to false edges; and the Accuracy. Table 2 presents for each of the four edge detectors, the Average and the Standard Deviation calculated to assess quantitatively the dispersion of the results for the 500 test images.

Table 2. Comparison of Approaches.

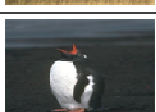|	Proposed Approach		Sobel		Prewitt		Canny	
	PR	Accuracy(%)	PR	Accuracy(%)	PR	Accuracy(%)	PR	Accuracy(%)
Average	13.32	97.12	10.05	95.72	10.14	95.65	11.75	96.32
Standard Deviation	4.5	0.75	3.95	0.74	3.89	0.84	4.4	0.85

Fig. 14 Comparison of edge detectors on the BSDS500. From left to right: Image No., BSDS Image, Ground Truth, Canny's approach, Prewitt's approach, Sobel's approach, proposed approach.

IJCSI International Journal of Computer Science Issues, Volume 12, Issue 1, No 2, January 2015
ISSN (Print): 1694-0814 | ISSN (Online): 1694-0784
www.IJCSI.org

20

The proposed approach resulted in the highest PR and Accuracy parameters compared to the reference edge detectors.

Examples of results are shown in fig. 14.

5. Conclusion

In this paper, a multiscale algorithm for the extraction of the most significant edges has been presented. The method proposes a robust multiscale edge detector preceded by a pre-processing step, mainly consisting of transformations to the desired color spaces; then followed by a choice of the most discriminating color space.

The edge detection is a critical phase in image processing. It was proven that the method presented in this paper has given good results in spite of its application on natural images, which are very complex. Also, the proposed method does not require any type of pre-filtering of the used images. The use of color image allows taking into consideration all the data in the image, while preserving most of the information, which is not the case when handling with gray images. The selection of the most discriminating color space step shows that YCbCr color space presents the closest edge maps to the Ground Truths. This phase allows deciding which color space is the best for the type of images used with this proposed method. This conclusion was based on the robust ROC analysis because it uses references done by experts. The proposed method is found to give better results on the studied images from Berkley database when using the YCbCr plan. The performance of the proposed flowchart was tested compared with Canny, Sobel and Prewitt edge detectors. Experimental results show that the proposed approach gives higher PR and Accuracy. It reduces the false edge detection and the double edges.

As an extension to this work, the determination of objects in color image can be performed.

References

[1] V. D. Noutsou, and D. P. A. Michalis, "Edge detection of manmade objects using wavelets in high resolution satellite images", in ASPRS Annual Conference Tampa., 2007, Vol. 1, pp. 7-11.

[2] C. G. HEALEY, and J. T. ENNS, "A perceptual colour segmentation algorithm", Tech. Rep. TR-96-xx, Department of Computer Science, University of British Columbia, 1996.

[3] P. Chauhan, and R. V Shahabade, "Edge detection comparison on various color spaces using histogram equalization", International Journal of Advanced Computational Engineering and Networking, Vol. 1, No. 4, 2013, pp. 7-10.

[4] N. Bassiou, and C. Kotropoulos, "Color image histogram equalization by absolute discounting back-off", Computer Vision and Image Understanding, Vol. 107, No. 1-2, 2007, pp. 108-122.

[5] C. L. Novak, and S. A. Shafer, "Color edge detection", in DARPA Image Understanding Workshop, 1987, Vol. 1, pp. 35-37.

[6] R. Nevatia, "A color edge detector and its use in scene segmentation", IEEE Trans. Syst., Man, Cybern., Vol. SMC-7, No. 11, 1977, pp. 820-826.

[7] M. Hedley, and H. Yan, "Segmentation of color images using spatial and color space information", Journal of Electronic Imaging, Vol. 1, No. 4, 1992, pp.374-380.

[8] T. Carron, and P. Lambert, "Color edge detector using jointly hue, saturation and intensity", in IEEE International Conference (ICIP94), 1994, Vol. 3, pp. 977-981.

[9] A. Bouzid, and N. Ellouze, "Voice source parameter measurement based on multi-scale analysis of electroglottographic signal", Speech Commun., Vol. 51, No. 9, 2009, pp. 782-792.

[10] A. Bouzid, and N. Ellouze , " Multiscale product of electroglottogram signal for glottal closure and opening instant detection", in Computational Engineering in Systems Applications, IMACS Multiconference on, 2006, Vol. 1, pp. 106-109.

[11] S. Mallat, and W.L. Hwang, "Singularity detection and processing with wavelets," IEEE Trans on Inform. Theory, Vol. 38, 1992, pp. 617-643.

[12] M. Kaur, and R. Mittal, "Survey of Intelligent Methods for Brain Tumor Detection," IJCSI International Journal of Computer Science Issues, Vol. 11, No 1, September 2014, pp. 108-117.

[13] B. M. Sadler, and A. Swami, "Analysis of multiscale products for step detection and estimation," Information Theory, IEEE Transactions on, Vol.45, No.3, Apr 1999, pp.1043-1051.

[14] S. Mallat, and W. L. Hwang, "Singularity detection and processing with wavelets," Information Theory, IEEE Transactions on, Vol.38, No.2, March 1992, pp.617-643.

[15] E. Prathibha, S. Yellampalli, and A. Manjunath, "Design and Implementation of Color Conversion Module RGB to YCbCr and Vice Versa", IJCSI International Journal of Computer Science Issues, Vol. 1, No 1, September 2011, pp. 13-18.

[16] W. Yue-Liang, C. Yuan-da, and L. Dun, "A Single Threshold Edge Detection Algorithm Based on Multiscale Fusion," in Computational Intelligence and Security, 2006 International Conference on , Vol. 2, No. , 2006, pp.1710-1715.

[17] C. S. Burrus, and H. Guo, "Introduction to wavelets and wavelet transforms", New Jersey: Prentice Hall Upper Saddle River, 1998.

[18] S.G. Mallat, A Wavelet Tour of Signal Processing, San Diego: Academic Press, 1998.

[19] S. Mallat, and S. Zhong, "Characterization of signals from multiscale edges," Pattern Analysis and Machine Intelligence, IEEE Transactions on, Vol.14, No.7, Jul 1992, pp.710-732.

[20] Y. Xu, J.B. Weaver, D. M. Healy, and J. Lu, "Wavelet transform domain filters: a spatially selective noise filtration technique", Image Processing, IEEE Transactions on, Vol. 3, No.6, 1994, pp.747-758.

[21] B. M. Sadler, and A. Swami, "Analysis of multiscale products for step detection and estimation", Information Theory IEEE Transactions on, Vol. 45, No. 3, 1999, pp.1043-1051.

[22] M. Tello Alonso, C. Lopez-Martinez, J. J. Mallorqui, and P. Salembier, "Edge Enhancement Algorithm Based on the Wavelet Transform for Automatic Edge Detection in SAR Images", Geoscience and Remote Sensing, IEEE Transactions on, Vol. 49, No. 1, 2011, pp. 222-235.

[23] D. Martin, C. Fowlkes, D. Tal, and J. Malik, "A database of human segmented natural images and its application to evaluating segmentation algorithms and measuring ecological statistics", in Computer Vision, 2001. ICCV 2001 Proceedings. Eighth IEEE International Conference on, Vol.2, No., 2001, pp.416-423.

[24] J. Egan, Signal detection theory and roc analysis, Academic Press Series in Cognitition and Perception, New York, USA, 1975.

[25] P. A. Khaire, and N. V. Thakur, "A Fuzzy Set Approach for Edge Detection", in International Journal of Image Processing (IJIP), 2012, Vol. 6, pp. 403-412.

[26] T. Stathaki, "Image Fusion - Algorithms and Applications", U.K: Academic Press, 2008.

[27] J. Canny, "A Computational Approach to Edge Detection", Pattern Analysis and Machine Intelligence IEEE Transactions on, Vol. PAMI-8, No. 6, Nov. 1986, pp.679-698.

[28] I.E. Sobel, "Camera Models and Machine Perception", PhD thesis, Stanford Univ., Stanford, CA, 1970.

[29] J. M. S. Prewitt, "Object enhancement and extraction," in Picture Processing and Psychopictorics, B. Limpkin and A. Rosenfeld, Eds. New York: Academic, 1970, pp. 75-149.

Sihem Charaâ is a PhD student in National Engineering High School of Tunis (ENIT). She earned her Bachelor degree in computer science from Sciences High University of Tunis, Tunisia, and her Master degree in Signal and image processing from National Engineering High School of Tunis. Her PhD is specializing in Image Processing.

Pr. Noureddine Ellouze received a PhD degree in 1977 from l'Institut National Polytechnique at Paul Sabatier University (Toulouse, France), and Electronic Engineer Diploma from ENSEEIHT in 1968 at the same university. He have served as Director of Electrical Department at ENIT from 1978 to 1983, General Manager and President of the Research Institute on Informatics and Telecommunications (IRSIT) from 1987 to 1990, President of the same Institute from 1990 to 1994. He is now Director of Signal Processing Research Laboratory (LSTS) at ENIT and is in charge of Control and Signal Processing Master degree at ENIT.
Pr. Ellouze is IEEE fellow since 1987, he directed multiple Master thesis and PhD thesis and published over 200 scientific papers in journals and conference proceedings. He is chief editor of the scientific journal Annales Maghrébines de l'Ingénieur. His research interests include Neural Networks and Fuzzy Classification, Pattern Recognition, Signal Processing and Image Processing applied in Biomedical, Multimedia, and Man Machine Communication.